Carbohydrate Polymers 100 (2014) 9–16

Contents lists available at ScienceDirect

Carbohydrate Polymers

journal homepage: www.elsevier.com/locate/carbpol

Changes in the cell wall and cellulose content of developing cotton fibers investigated by FTIR spectroscopy

Noureddine Abidi[a,*], Luis Cabrales[a], Candace H. Haigler[b]

[a] Fiber and Biopolymer Research Institute, Department of Plant and Soil Science, Texas Tech University, Lubbock, TX, USA
[b] Department of Plant Biology and Department of Crop Science, North Carolina State University, Raleigh, NC, USA

ARTICLE INFO

Article history:
Received 16 August 2012
Received in revised form 11 January 2013
Accepted 24 January 2013
Available online 1 February 2013

Keywords:
Cellulose
FTIR
Cotton
Fiber development
Maturity
Cell wall

ABSTRACT

Fourier transform infrared (FTIR) spectra of cotton fibers harvested at different stages of development were acquired using Universal Attenuated Total Reflectance FTIR (UATR-FTIR). The main goal of the study was to monitor cell wall changes occurring during different phases of cotton fiber development. Two cultivars of *Gossypium hirsutum* L. were planted in a greenhouse (Texas Marker-1 and TX55). On the day of flowering, individual flowers were tagged and bolls were harvested. From fibers harvested on numerous days between 10 and 56 dpa, the FTIR spectra were acquired using UATR (ZnSe-Diamond crystal) with no special sample preparation. The changes in the FTIR spectra were used to document the timing of the transition between primary and secondary cell wall synthesis. Changes in cellulose during cotton fiber growth and development were identified through changes in numerous vibrations within the spectra. The intensity of the vibration bands at 667 and 897 cm^{-1} correlated with percentage of cellulose analyzed chemically.

1. Introduction

Fourier transform infrared microspectroscopy (FTIR) has emerged as a versatile and important analytical technique to study plant growth and development (Dokken, Davis, & Marinkovic, 2005). This is attributed mainly to the recent technological advances in FTIR instrumentation. Indeed, the development of attenuated total reflectance (ATR) has made this technique very easy to use and reduced the sampling time. The ATR crystal is usually made of ZnSe, Ge, or diamond. Using UATR-FTIR, samples such as a bundle of cotton fibers can be analyzed in few seconds. The use of ATR allows the analysis of samples in their original states and environments. This technique has replaced the traditional KBr pellet technique.

FTIR has been used in many previous investigations of plant cell wall composition and organization. McCann et al. reported that FTIR spectroscopy provides a powerful and rapid assay for cell wall components and putative cross-links by identifying polymers and functional groups nondestructively in muro (McCann, Hammouri, Wilson, Belton, & Roberts, 1992). FTIR microspectroscopy of dry and dehydrated walls of single epidermal cells showed that IR bands associated with pectin or cellulose were stronger with polarization perpendicular or parallel to the direction of the cell elongation, respectively (Chen, Wilson, & McCann, 1997). Others acquired polarized one and two-dimensional infrared spectra from the epidermis of onion under hydrated and mechanically stressed conditions, demonstrating that cellulose and pectin exhibited little orientation until imposed mechanical stress induced their reorientation (Wilson et al., 2000).

In flax stems, FTIR microspectroscopy showed that xylem differentiation was accompanied by re-esterification of pectin and increased lignification, whereas cellulose predominated in the fiber cell walls (Stewart, Mcdougall, & Baty, 1995). A study of the cotton seed coat using the same technique also showed differences in individual cell walls within tissues. Among 5 layers in the seed coat (described as epidermal, outer pigmented, colorless, palisade, and inner pigmented) FTIR analysis showed: cutin, wax, cellulose, and pectin in the epidermal layer; pectin, hemicellulose, and aromatic molecules including polyphenols in the palisade layer; and predominantly lignin in the outer and inner pigmented layers (Yan et al., 2009).

FTIR spectroscopy has been used in conjunction with principal component analysis (PCA) and linear discriminant analysis (LDA) to detect and classify a broad range of cell-wall mutants from a large mutagenized *Arabidopsis* population (Chen et al., 1998). Similarly, transmission spectra generated with FTIR microspectroscopy were statistically analyzed to identify and classify *Arabidopsis* cell wall mutants generated through drug treatments (Mouille, Robin, Lecomte, Pagant, & Hofte, 2003).

* Corresponding author at: PO Box 45019, Lubbock, TX 79409, USA. Tel.: +1 806 742 5333; fax: +1 806 742 5343.
E-mail address: n.abidi@ttu.edu (N. Abidi).

0144-8617/$ – see front matter © 2013 Elsevier Ltd. All rights reserved.
http://dx.doi.org/10.1016/j.carbpol.2013.01.074

The cell walls analyzed in the current research were from developing cotton fiber, an elongated seed epidermal cell with a thickened secondary cell wall (SCW) composed of nearly pure cellulose (Haigler, Betancur, Stiff, & Tuttle, 2012). The day of flowering is defined as anthesis and the term days post anthesis (dpa) is used to describe the temporal progression of fiber development (Haigler et al., 2012). There is a continuous change in the composition of the cell wall throughout cotton fiber development (Meinert & Delmer, 1977). The composition of cotton fiber cell wall extracts has been extensively analyzed (Gokani, Kumar, & Thaker, 1998; Huwyler, Franz, & Meier, 1979; Maltby, Carpita, Montezinos, Kulow, & Delmer, 1979; Meinert & Delmer, 1977; Timpa & Triplett, 1993; Tokumoto, Wakabayashi, Kamisaka, & Hoson, 2002), but limited research has been conducted on intact fibers before processing. The usefulness of UATR-FITR for analyzing dynamic changes in cotton fiber cell walls has been demonstrated before (Abidi et al., 2008; Abidi, Cabrales, & Hequet, 2010; Abidi, Hequet, & Cabrales, 2010). Specifically, the authors reported that the evolution of the integrated intensities of specific vibrations observed at 1733, 1534, and 1627 cm^{-1} over fiber developmental time could be used to monitor the progress of cellulose deposition in cotton fibers. In this paper, we report on the use of the UATR-FTIR to study the changes occurring during different phases of fibers development from 10 dpa until 56 dpa in two cotton cultivars.

2. Experimental

2.1. Materials

Two cotton cultivars of *Gossypium hirsutum* L. were selected for this study. Texas Marker-1 (TM-1) is the standard reference for American Upland cotton (Kohel, Richmond, & Lewis, 1970). TX55 cultivar was analyzed in previous research (Abidi et al., 2008; Abidi, Cabrales, et al. 2010; Abidi, Hequet, et al. 2010). Two independent replications (10 plants each) were planted in a greenhouse with 11–13 h days and a diurnal temperature cycle about 31 °C/24 °C. Plants were grown in 20 liters (5 gallons) pots of Sungrow SB 300 potting mix that had been amended with Peters 15-9-12 slow release fertilizer prior to potting. Plants were watered as needed. On the day of flowering (0 dpa), individual flowers were tagged, and 14 developing bolls per cultivar and per replication were harvested at 10, 14, 17, 18, 19, 20, 21, 22, 23, 24, 27, 30, 36, 46, and 56 dpa. The pericarp was immediately removed (excised with scalpel) and isolated ovules were transferred into cryogenic vials and stored in a Cryobiological Storage System filled with liquid nitrogen prior to analysis.

2.2. Methods

2.2.1. Sample dehydration

Cotton ovules were thawed and the fibers were separated from the seeds and rinsed with distilled water several times to remove sugars and other water-soluble compounds. Cotton fibers obtained from several bolls were mixed by hand. The fibers were dried at 40 °C for 2 days and conditioned in a laboratory maintained at 21 ± 1 °C and 65 ± 2% relative humidity for at least 2 days prior to FTIR analysis.

2.2.2. FTIR measurements

The FTIR spectra of cotton fiber samples were recorded under environmentally controlled conditions as specified above using an FTIR instrument (Spotlight 400) equipped with an UATR accessory (PerkinElmer, USA). The UATR-FTIR was also equipped with a ZnSe-Diamond crystal composite (1 bounce) that allows collection of FTIR spectra directly on a sample without any special preparation. The "pressure arm" of the instrument was used to apply a constant pressure (monitored by software) to the cotton samples positioned on top of the ZnSe-Diamond crystal to ensure a good contact between the sample and the incident IR beam, thereby minimizing loss of the IR beam. A total of 5400 FTIR spectra were acquired: 2 cultivars × 15 dpa × (30 spectra × 3 technical replications) × 2 independent greenhouse growth replications. All FTIR spectra were collected at a spectrum resolution of 4 cm^{-1}, with 32 co-added scans over the range from 4000 cm^{-1} to 650 cm^{-1}. A background scan of the clean ZnSe-Diamond crystal was acquired before scanning the samples.

2.2.3. FTIR spectra analysis

The Perkin-Elmer software was used to perform spectra normalization, baseline corrections, and peak integration (Spectrum V. 6.2.0, 2007). Principal component analysis (PCA) with leverage correction and mean-center cross validation boxes checked was performed using Unscrambler V.9.6 Camo Software AS (CAMO Software AS, Norway).

2.2.4. Cellulose content determination

Cellulose content of developing cotton fibers was determined using the anthrone method (Viles & Silverman, 1949). Anthrone, a tricyclic hydrocarbon ($C_{14}H_{10}O$), is generally used for colorimetric determination of carbohydrates, including cellulose. Sample preparation for the cellulose content determination was performed as followed: for fibers from 10 to 21 dpa, fibers were first chopped at 12,000–17,000 rpm in a homogenizer (Pro200 Homogenizer with 7 mm generator, PRO Scientific, CT). The solution was centrifuged and the supernatant water was discarded. The samples were then rinsed with DI water and twice with acetone, and finally dried at 105 °C for 1 day. For fibers from 22 to 56 dpa, samples were chopped in a Wiley Mill to pass through a 20 mesh screen and then dried at 105 °C for 1 day. Between 0.01 to 0.05 g dried fiber was digested in acetic nitric reagent (Updegraff, 1969) to remove most of the non-cellulosic components, followed by hydrolysis with 67% H_2SO_4 (1 h, RT) to release glucose. Anthrone (0.20%) in concentrated sulfuric acid was added, and the absorbance (625 nm) was proportional to the cellulose content of the sample. Microcrystalline cellulose (Avicel PH102; FMC Biopolymer, USA) was used as a standard for the calibration.

3. Results and discussion

Typical FTIR spectra of fibers from TM-1 cultivar harvested at different stages of development showed different vibrations (with assignments in Table 1) that changed in location and/or intensity with fiber development (Fig. 1). As widely used before (Abidi, Cabrales, et al. 2010; Abidi, Hequet, et al. 2010; Chen et al., 1998; Mouille et al., 2003), PCA analysis helped to reduce the dimensionality of the original spectral data from thousands of variables (3350 wavenumbers) to fewer dimensions. The variability in each spectrum relative to the mean of the population was represented as a smaller set of values (axes), termed principal components (PCs). The main sources of variability in the data were concentrated into the first 2 PCs (PC1 and PC2), and the scores for PC1 vs PC2 were plotted against each other to show relationships between spectra over fiber developmental time. For TM-1 fiber (Fig. 2a), PC1 accounts for 90% of the variance and clearly separates the FTIR spectra into three groups: group 1 derived from 10 to 21 dpa fiber, group 2 derived from 22 to 30 dpa fiber, and group 3 derived from 36 to 56 dpa fiber. For TX55 fiber (Fig. 2b), PC1 accounts for 86% of the variance and clearly separates the FTIR spectra into three groups: group 1 derived from 10 to 18 dpa fiber, group 2 derived from 19 to 30 dpa fiber, and group 3 derived from 36 to 56 dpa fiber. Based on the typical progression of cotton fiber development (reviewed in Haigler et al., 2012) and other results in this paper, these groups

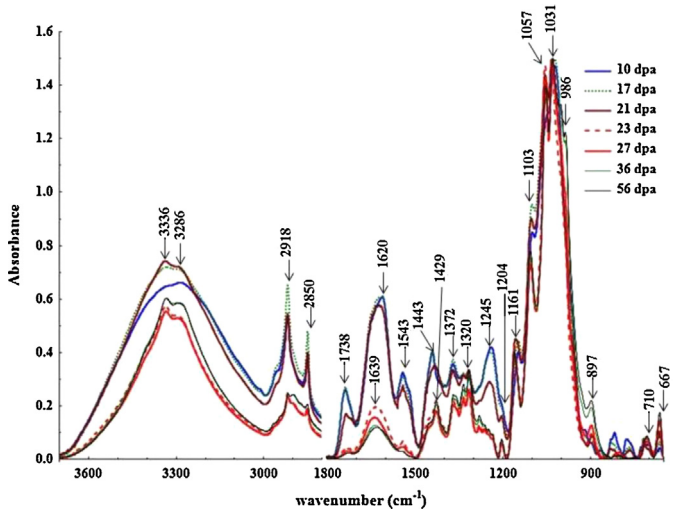

Fig. 1. UATR-FTIR spectra of fibers from TM-1 harvested at different developmental stages. The IR region between 1800 and 2800 cm^{-1} has been omitted from the spectra because it does not contain any significant bands.

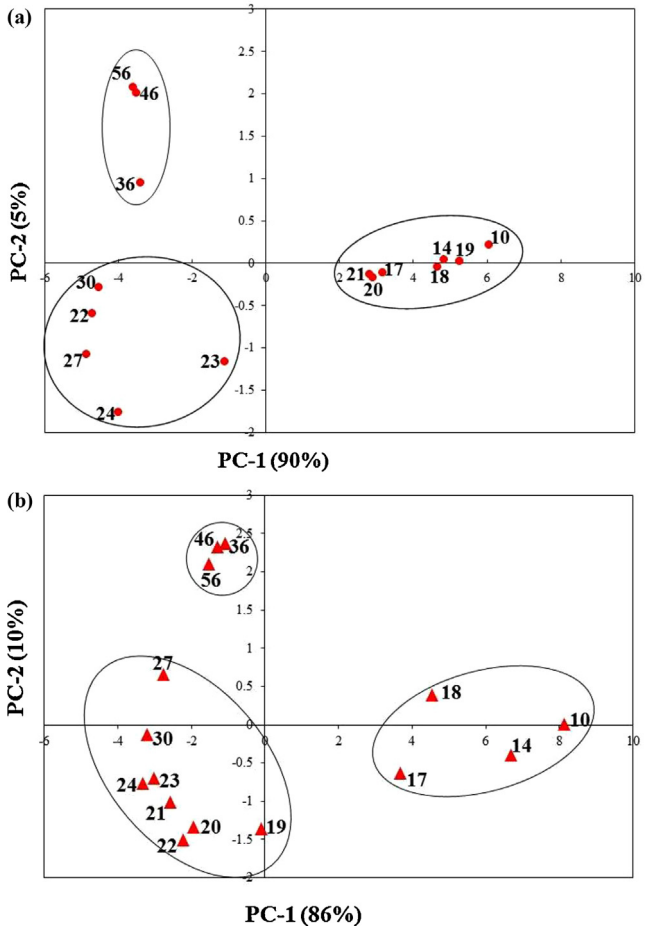

Fig. 2. (a) Principal component analysis of FTIR spectra of fibers from TM-1 separates the spectra in three groups: group 1 representing 10–21 dpa fiber; group 2 representing 22–30 dpa fiber; and group 3 representing 36–56 dpa fiber. (b) Principal component analysis of FTIR spectra of fibers from TX55 separates the spectra in three groups: group 1 representing 10–18 dpa fiber; group 2 representing 19–30 dpa fiber; and group 3 representing 36–56 dpa fiber.

Table 1
IR assignments of the main vibrations in the FTIR spectra.

IR region (cm^{-1})	Vibrations (cm^{-1})	Assignments
3700–3000	3336	Intra-molecular hydrogen bonding C(3)OH···O(5) C(6)O···(O)H
	3286	Inter-molecular hydrogen bonding C(3)OH···C(6)O
3000–2800	2918, 2850	CH_2 asymmetrical and symmetrical stretching
1800–1500	1738	C=O stretching
	1639	O—H bending of adsorbed water
	1620	C=O (amide I)
	1543	NH_2 deformation
1500–1200	1443	O—H in-plane deformation
	1429	CH_2 scissoring
	1372	C—H bending
	1315	CH_2 rocking
	1245	C=O stretching or NH_2 deformation
	1204	C—O stretching
1200–650	1161	Anti-symmetrical bridge C—O—C stretching
	1100	Anti-symmetric in-plane stretching band
	1056	C—O stretch
	1018	C—O stretch
	1003, 986	C—O and ring stretching modes
	897	β-Linkage of cellulose
	710	CH_2 rocking
	667	OH out-of-plane bending

are generally associated with: group 1, fiber elongation via primary wall synthesis; group 2, synthesis of the winding cell wall layer (analogous to the S1 layer in wood fiber) followed by secondary wall cellulose synthesis; and group 3 ending of secondary wall thickening and fiber maturation. Possibly, TX55 is undergoing the transition to secondary wall cellulose synthesis along with the end of fiber elongation a few days earlier than TM-1.

3.1. IR region 3700–3000 cm^{-1}

The broad band in this region is due to the OH-stretching vibrations arising from hydrogen bonding in cellulose. One of two main vibrations, at 3336 cm^{-1}, became visible starting at 20 dpa, and it is assigned to intra-molecular hydrogen bonding of cellulose (between C(3)OH···O(5) and C(6)O···O(2)H) (Oh, Yoo, Shin, & Seo, 2005; Oh et al., 2005; Schwanninger, Rodrigues, Pereira, & Hinterstoisser, 2004). The other main vibration, at 3286 cm^{-1}, was evident in all spectra starting at 10 dpa, and it is assigned to inter-molecular hydrogen bonding of cellulose (between C(3)OH···C(6)O) (Oh, Yoo, et al. 2005; Oh et al., 2005; Schwanninger et al., 2004).

The evolution of the integrated intensity of the vibrations observed at 3336 cm^{-1} and 3286 cm^{-1} ($I_{3336+3286}$) was calculated between 3700 and 3000 cm^{-1} and reported as function of dpa for both TM-1 and TX55 fibers (Fig. 3). The analysis of variance shows statistically significant effects of the fiber developmental stages ($F(14,30) = 23.254$, $p = 0.000001$), the cultivar ($F(1,30) = 18.355$, $p = 0.0002$), and the dpa*cultivar interaction ($F(14,30) = 2.634$, $p = 0.0127$). The major difference in $I_{3336+3286}$ between cultivars occurs from 18 to 27 dpa. Overall, three regions of $I_{3336+3286}$ values occur: region I between 10 and 19 dpa; region II between 20 and 30 dpa (a time of rapid change); and region III between 36 and 56 dpa. Region I corresponds to the period of primary cell wall synthesis to support fiber elongation, which typically continues linearly until about 20 dpa in *G. hirsutum* (Tokumoto

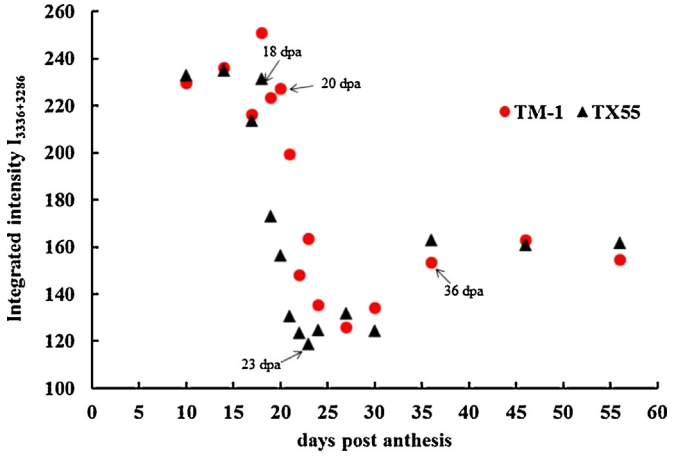

Fig. 3. Integrated intensity of the vibrations located at 3336 cm^{-1} (reflecting cellulose intra-molecular hydrogen bonding between C(3)OH···O(5) and between C(6)O···O(2)H) and 3286 cm^{-1} (reflecting cellulose inter-molecular hydrogen bonding between C(3)OH·····C(6)O) as a function of days post anthesis. Three regions in the data were present: Region I, 10–19 dpa, representing the primary cell wall and fiber elongation phase; Region II, 20–30 dpa, representing fiber wall thickening, largely due to cellulose synthesis; and Region III, 30–56 dpa, fiber maturation.

et al., 2002). Region II corresponds to the transition phase and SCW development. During this time, the fiber wall thickens, first by winding layer synthesis then through nearly pure cellulose synthesis (Haigler et al., 2012). Region III corresponds to the period of fiber maturation after SCW cellulose synthesis is completed, typically about 32 dpa (Meinert & Delmer, 1977; see also Table 2).

3.2. IR region 3000–2800 cm^{-1}

This region contains two vibrations at 2918 and 2850 cm^{-1}, which are assigned to CH_2 asymmetrical and symmetrical stretching, respectively (Abidi, Cabrales, et al. 2010; Abidi, Hequet, et al. 2010; Nelson & Mares, 1965). These vibrations are sharp at 10–22 dpa and 10–18 dpa for TM-1 and TX55, respectively. After washing out soluble sugars, the fiber residue contains proteins, pectic molecules, and wax (Nelson & Mares, 1965). The intensities of the 2918 and 2850 cm^{-1} vibrations decrease in the FTIR spectra of fibers harvested after 23 dpa or 19 dpa from TM-1 and TX55, respectively. This is attributed to the fact that loss of particular primary wall components, including pectin, occurs at the transition stage (Singh et al., 2009) followed by the dominance of secondary wall cellulose (Abidi et al., 2008) so that noncellulosic materials are no longer detected (Nelson & Mares, 1965).

3.3. IR region 1800–1500 cm^{-1}

This region contains four main vibrations at 1738, 1639, 1620, and 1543 cm^{-1}. The vibration at 1738 cm^{-1} is attributed to C=O stretching, probably within esterified uronic acid (Alonso-Simon et al., 2011; McCann et al., 1992). The vibration at 1639 cm^{-1} is assigned to O—H bending of adsorbed water (Abidi et al. 2008; Abidi, Cabrales, & Hequet, 2010; Abidi, Hequet, & Cabrales, 2010; Schwanninger et al., 2004). The vibration at 1620 cm^{-1} is assigned to C=O (amide I), which could originate from protein or pectic acid ester (Nelson & Mares, 1965). The vibration at 1543 cm^{-1} is assigned to amide II (proteins, amino acids) (Kong & Yu, 2007).

The integrated intensity of the 1738 cm^{-1} vibration was calculated between 1800 and 1700 cm^{-1} and reported as function of dpa (Fig. 4). The analysis of variance shows statistically significant effects of the developmental stages ($F(14,30) = 75.4336$, $p = 0.000001$) and cultivar ($F(1,30) = 26.4853$, $p = 0.000015$), but no dpa*cultivar interaction. The results are consistent with an initially high concentration of esterified uronic acids at 10 dpa continuously decreasing through 24 dpa, after which the 1738 cm^{-1} vibration became undetectable. Consistently, chemical analysis of total uronic acids in the cotton fiber cell wall showed a decrease from 22% to 2% (wt/wt) from 10 to 22 dpa (Meinert & Delmer, 1977). More specifically, the results are consistent with the de-esterification of pectin as a restrictor of cotton fiber elongation (Haigler et al., 2012).

Table 2
Schematic of the changes in the FTIR bands' intensities and cellulose content as a function of the fiber age (days post anthesis). Levels of the vibration intensity are indicated by a color code: red, high; yellow, a period of rapid change; green, intermediate; blue, low; and gray, no change relative to the prior day. The peach color demarcates groups only without respect to levels.

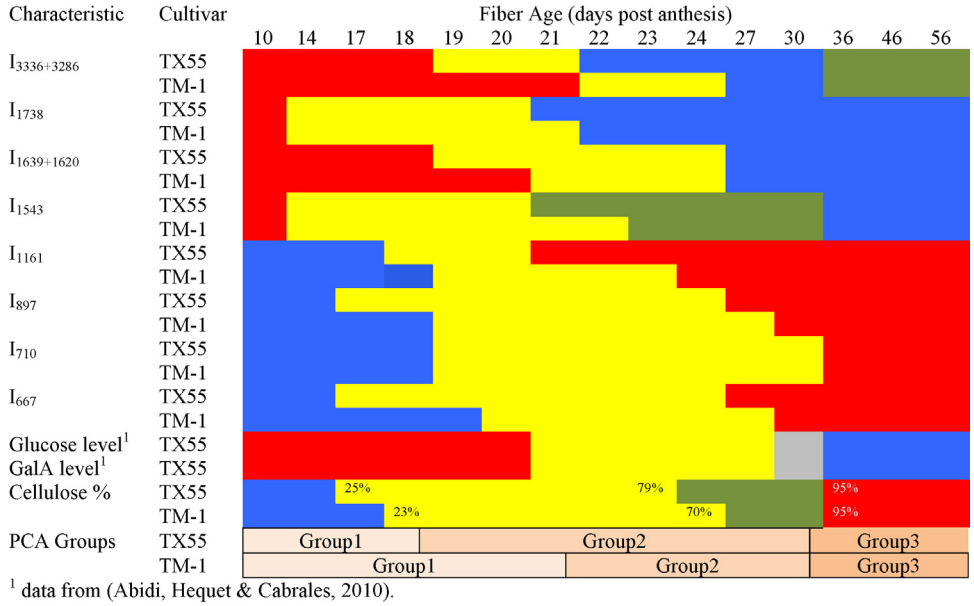

[1] data from (Abidi, Hequet & Cabrales, 2010).

GalA: Galacturonic acid

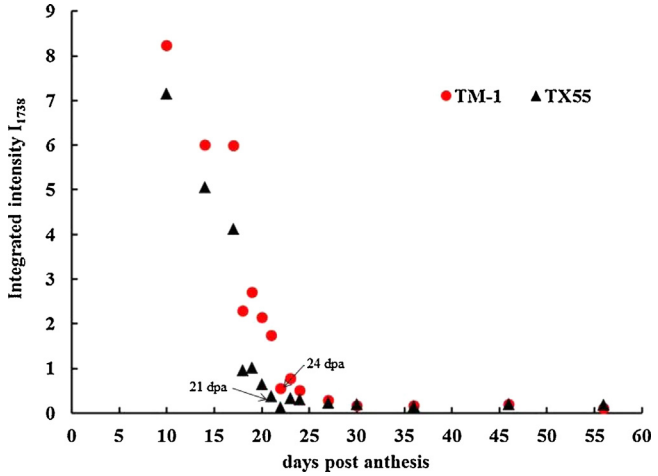

Fig. 4. Integrated intensity of the 1738 cm^{-1} vibration (C═O stretching, esterified uronic acid) as a function of days post anthesis indicating a high concentration of esterified uronic acids at 10 dpa followed by a continuous decrease until 24 dpa.

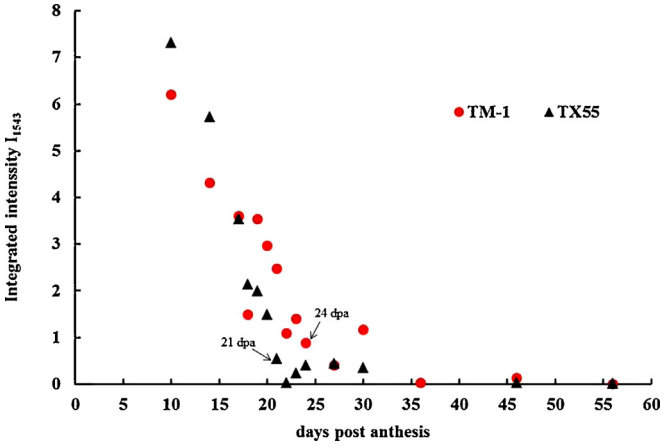

Fig. 6. Integrated intensity of the 1543 cm^{-1} vibration (NH_2 deformation, proteins and/or amino acids) as a function of days post anthesis. The pattern of signal intensity was consistent with a high percentage of proteins and/or amino acids at 10 dpa, followed by a continuous decrease until 30 dpa. The signal became undetectable after 36 dpa.

The IR region between 1700 and 1560 cm^{-1} shows two peaks at 1639 and 1620 cm^{-1}, and the integrated intensity ($I_{1639+1620}$) was graphed as a function of dpa (Fig. 5). The analysis of variance shows statistically significant effects of the developmental stages ($F(14,30) = 50.546$, $p = 0.000001$), cultivar ($F(1,30) = 14.065$, $p = 0.0008$), and the dpa*cultivar interaction ($F(14,30) = 2.629$, $p = 0.0129$). The $I_{1639+1620}$ intensity also decreased sharply until 24 dpa.

The integrated intensity of the 1543 cm^{-1} (I_{1543}) vibration was calculated from 1560 and 1485 cm^{-1} (Fig. 6). The analysis of variance shows statistically significant effects of the developmental stages ($F(14,30) = 46.7376$, $p = 0.000001$), the dpa*cultivar interaction ($F(14,30) = 2.7672$, $p = 0.0094$), and the cultivar ($F(1,30) = 6.0683$, $p = 0.0197$). Overall, I_{1543} decreased continuously until 22 dpa and became undetectable in fibers harvested at 36 dpa and afterwards.

3.4. IR region 1500–1200 cm^{-1}

This region contains six vibrations of interest. The 1443 cm^{-1} vibration could be assigned to O—H in-plane deformation and it was sharp in 10–21 dpa fibers but only appeared as a small shoulder in the FTIR spectra of 21–56 dpa fibers. If this band relates to CH_2 scissoring (Nelson & Mares, 1965), it may shift from 1443 cm^{-1} to 1429 cm^{-1} between 21 and 56 dpa. Alternatively, the vibration 1429 cm^{-1} has been designated as a "crystalline" absorption band, with its ratio with the 897 cm^{-1} vibration defined as an empirical "crystallinity index" of cellulose (Krassig, 1993).

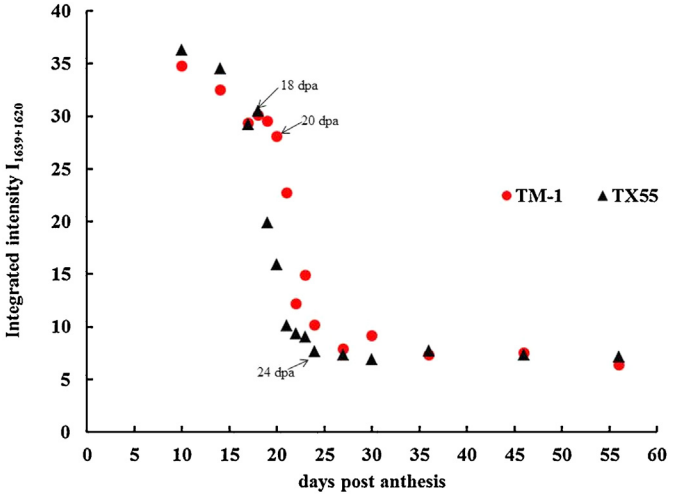

Fig. 5. Integrated intensity of the vibrations located at 1639 cm^{-1} (O—H bending of adsorbed water) and 1620 cm^{-1} (C═O, pectins) as a function of days post anthesis showing a continuous decrease until 24 dpa.

The 1372 cm^{-1} vibration is assigned to C—H bending, and it may be most suitable for indicating cellulose crystallinity in ratio with the 2900 cm^{-1} vibration (Nelson & O'Connor, 1964). In developing cotton fibers, the 1372 cm^{-1} vibration exists as a small shoulder at early dpa then becomes a sharp peak starting at 22 dpa. Similarly, the 1315 cm^{-1} vibration, which is assigned to CH_2 rocking (Schwanninger et al., 2004), existed only as a small shoulder in the FTIR spectra from 10 to 22 dpa but became stronger afterwards. The 1204 cm^{-1} vibration, which is assigned to the C—O stretching mode of the pyranose ring (Ilharco, Garcia, daSilva, & Ferreira, 1997; Pastorova, Botto, Arisz, & Boon, 1994), behaved similarly. Conversely, the 1245 cm^{-1} vibration is assigned to C═O stretching or NH_2 deformation (pectic substances, amino acids) (Nelson & Mares, 1965), and it was strong between 10 and 22 dpa, becoming only a small shoulder in the FTIR spectra of older fibers. Overall the results for vibrations between 1500 and 100 cm^{-1} were consistent with the increasing dominance of secondary wall cellulose after 22 dpa.

3.5. IR region 1200–650 cm^{-1}

The 1145 cm^{-1} vibration is attributed to C—O—C stretching and could originate from non-cellulosic molecules, such as arabinogalactan or pectin (Kacurakova, Capek, Sasinkova, Wellner, & Ebringerova, 2000). The 1161 cm^{-1} vibration is attributed to anti-symmetrical bridge C—O—C stretching (Liang & Marchessault, 1959; Salmen & Bergstrom, 2009), particularly within cellulose (Alonso-Simon et al., 2011; Carpita et al., 2001; Kacurakova et al., 2000; Wilson et al., 2000). The integrated intensity of this vibration was calculated between 1185 and 1137 cm^{-1}, and a sharp 77% increase in its intensity occurs between 19 and 27 dpa (Fig. 7). The analysis of variance showed statistically significant effects of the developmental stages ($F(14,30) = 60.06$, $p = 0.000001$), cultivar ($F(1,30) = 37.33$, $p = 0.000001$), and the dpa*cultivar interaction ($F(14,30) = 3.90$, $p = 0.0008$).

The 1100 cm^{-1} vibration is assigned to anti-symmetric in-plane stretching (Ilharco et al., 1997), and it shifted to 1106 cm^{-1} at 23 dpa. The 1056 cm^{-1} vibration is attributed to C—O stretching

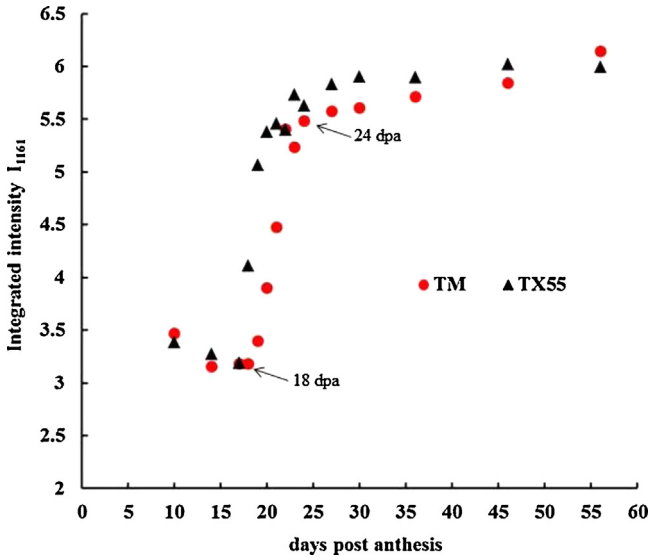

Fig. 7. Integrated intensity of the 1161 cm^{-1} vibration (antisymmetric bridge C—O—C stretching, cellulose) as a function of days post anthesis indicating that a large increase in the peak intensity occurs between 19 and 27 dpa.

mode (Abidi et al., 2008; Abidi, Cabrales, & Hequet, 2010; Abidi, Hequet, & Cabrales, 2010), and it existed only as a small shoulder in the FTIR spectra of fibers harvested at 10–17 dpa. The 1018 cm^{-1} vibration, attributed to C—O stretch, existed as a broad peak from 10 to 17 dpa then shifted to 1031 cm^{-1} in the FTIR spectra of fibers harvested after 18 dpa. The vibrations at 1003 and 986 cm^{-1}, which are attributed to C-O and ring stretching modes, appeared at 36 dpa.

The 897 cm^{-1} vibration is assigned to the β-linkage of cellulose (Alonso-Simon et al., 2011), and its integrated intensity (I_{897}) was calculated between 916 and 845 cm^{-1} (Fig. 8). The analysis of variance showed statistically significant effects of the developmental stages ($F(14,30) = 108.555$, $p = 0.000001$), the cultivar ($F(1,30) = 47.928$, $p = 0.000001$), and the dpa*cultivar interaction ($F(14,30) = 2.961$, $p = 0.0062$). Between 10 and 17 dpa, the 897 cm^{-1} peak is only a small shoulder, then I_{897} increases from 18 to 36 dpa. This pattern reflects cell wall thickening via enriched cellulose synthesis during this time, which is directly shown by the parallel increase in the percentage of cellulose (from <20% to

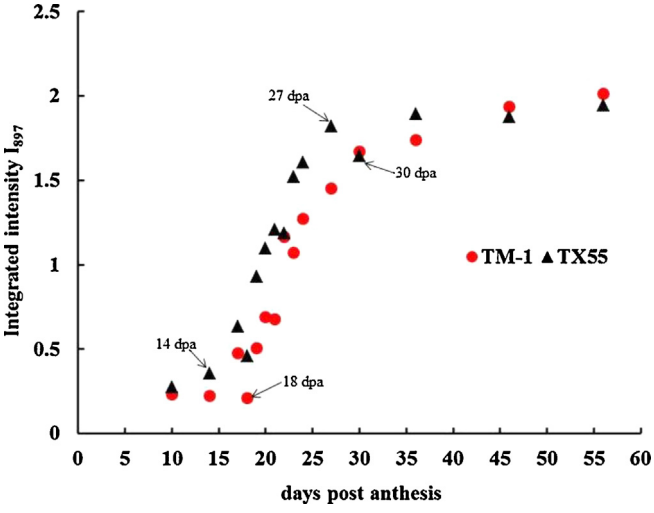

Fig. 8. Integrated intensity of the 897 cm^{-1} vibration (β-linkage, cellulose) as a function of days post anthesis showing that the increase of I_{897} begins at 18 dpa and levels off at 36 dpa.

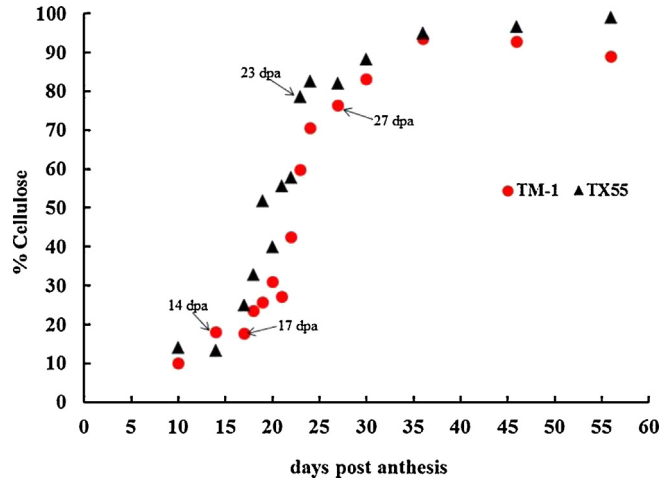

Fig. 9. Cellulose content in fibers from TM-1 and TX55 as a function of days post anthesis. Between 10 and 17 dpa, the cellulose content is less than 20%. The large increase in cellulose content occurs between 18 and 36 dpa.

> 83%) in the same time interval (Fig. 9). For cellulose content, the analysis of variance shows statistically significant effects of the developmental stages ($F(14,30) = 32.018$, $p = 0.000001$) and cultivar ($F(1,30) = 25.029$, $p = 0.00002$), but the dpa*cultivar interaction is not significant ($F(14,30) = 1.304$, $p = 0.2600$). There was a strong linear relationship ($R^2 = 0.95$) between cellulose content and I_{897} (Fig. 10), which demonstrates that cotton fiber cellulose content can be estimated indirectly from its FTIR spectrum.

The 710 cm^{-1} vibration is assigned to CH_2 rocking in crystalline cellulose I_β (Akerholm, Hinterstoisser, & Salmen, 2004). The integrated intensity (I_{710}) was calculated between 735 and 684 cm^{-1}, and it began to increase at 18 dpa (Fig. 11). Consistently, the degree of cellulose crystallinity increased from 30 to 58%, between 21 and 60 dpa, with the most increase occurring between 21 to 34 dpa (Hu & Hsieh, 1996). The analysis of variance of the I_{710} values shows statistically significant effects of the developmental stages ($F(14,30) = 32.018$, $p = 0.000001$) and the dpa*cultivar interaction ($F(14,30) = 2.262$, $p = 0.0298$), but no effect of the cultivar ($F(1,30) = 0.251$, $p = 0.6197$). The increase of I_{710} starting at 18 dpa indicates that cotton fibers, as they develop, become enriched in cellulose I_β. The primary wall of cotton fiber contains cellulose

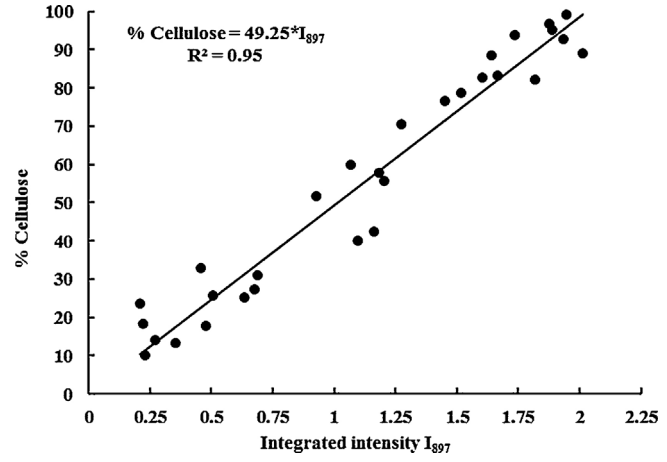

Fig. 10. Relationship between the cellulose content and the integrated intensity of the 897 cm^{-1} vibration. The strong linear relationship shows that I_{897} is useful for indirect estimation of the cellulose content in cotton fibers.

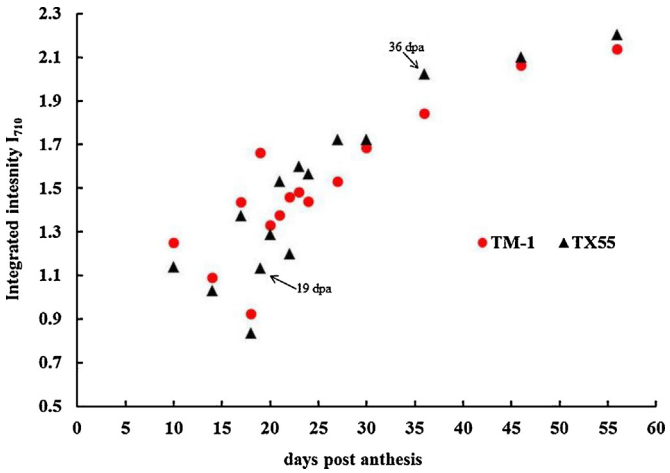

Fig. 11. Integrated intensity of the 710 cm^{-1} vibration (CH_2 rocking) as a function of days post anthesis. I_{710} increases starting at 18 dpa.

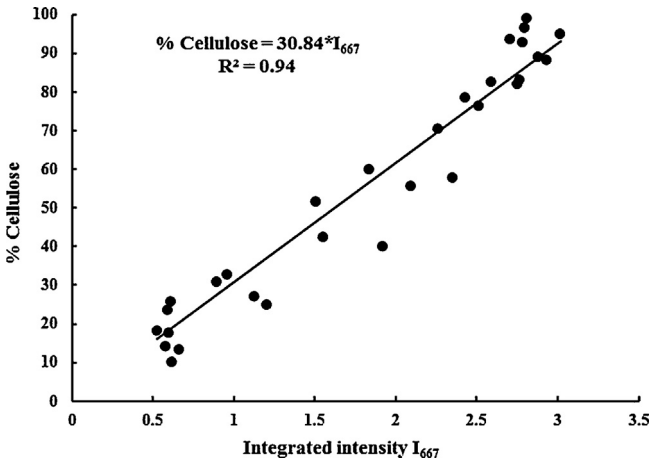

Fig. 13. Relationship between the cellulose content and the integrated intensity of the 667 cm^{-1} vibration. The strong linear relationship shows that I_{667} is useful for indirect estimation of the cellulose content in cotton fibers.

microfibrils with less lateral order than in the secondary wall (Chanzy, Imada, & Vuong, 1978), which is now thought to reflect a less organized form of the cellulose I_β allomorph within small cellulose fibrils (Wada, Heux, & Sugiyama, 2004). The secondary wall of mature cotton fiber is predominantly cellulose I_β (Atalla & VanderHart, 1984), implying that the organization of cellulose increases in the secondary wall.

The 667 cm^{-1} vibration is assigned to OH out-of-plane bending (Ilharco et al., 1997). The integrated intensity of this vibration (I_{667}) was calculated between 684 cm^{-1} and 650 cm^{-1} and reported as function of dpa (Fig. 12). For TX55 fibers, no major change in I_{667} occurred between 10 and 14 dpa, but between 17 and 36 dpa a 5-fold increase occurred. For TM-1 fibers, the increase in I_{667} occurred over a shorter period (19 to 30 dpa). The analysis of variance of I_{667} shows statistically significant effects of the developmental stages ($F(14,30) = 59.656$, $p = 0.000001$), cultivar ($F(1,30) = 37.143$, $p = 0.000001$), and the dpa*cultivar interaction ($F(14,30) = 2.762$, $p = 0.0096$). As already demonstrated for I_{897} (Fig. 10), there was a strong linear relationship ($R^2 = 0.94$) between cellulose content and I_{667} (Fig. 13), which demonstrates that cotton fiber cellulose content can be estimated indirectly from two FTIR bands (897 and 667 cm^{-1}).

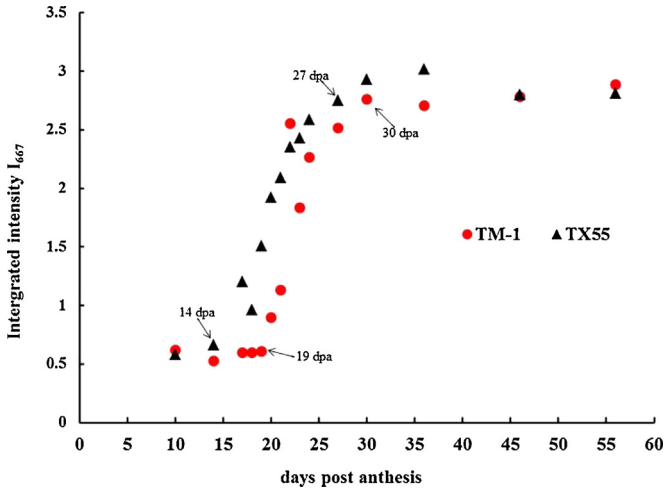

Fig. 12. Integrated intensity of the 667 cm^{-1} vibration (OH out-of-plane bending mode) as a function of days post anthesis. The strong increase in I_{667} occurs at 17 dpa for TX55 fibers and at 19 dpa for TM-1 fibers.

4. Conclusions

Particular vibrations in the FTIR spectrum are useful for characterizing changes in cellulose within developing cotton fibers (at 10 to 56 dpa) in two cultivars (Texas Marker-1 and TX55) grown in the greenhouse. Using Universal Attenuated Total Reflectance FTIR in the mid-IR, spectra were acquired directly on a bundle of fibers that had been rinsed in water, dried at 40 °C for 2 days, and finally conditioned to 21 ± 1 °C and 65 ± 1% RH for at least 2 days prior to analysis. Table 2 summarizes the data as the changes in the intensity of various FTIR bands and cellulose content during cotton fiber development. A color code of red, green, and blue was used to indicate high, moderate, and low levels of each parameter, respectively. The colors yellow and gray indicate rapid and no changes relative to the prior day, respectively. The clustering of the three groups from the PCA analysis of FTIR spectra are indicated in peach color without respect to levels. Our results showed that the integrated intensities of the vibrations observed at 3286, 1738, 1639, 1543, 1161, 897, 710, and 667 cm^{-1} are useful indicators of the deposition of secondary wall cellulose. There was an excellent correlation between the integrated intensities of the vibrations observed at 897 and 667 cm^{-1} and the cellulose content, which provides a relatively easy means of estimating cotton fiber cellulose content indirectly.

Acknowledgments

The authors would like to thank the Texas Department of Agriculture/Food and Fibers Research Grant Program and Cotton Incorporated/Texas State Support Committee for providing the financial support for this project.

References

Abidi, N., Cabrales, L., & Hequet, E. (2010). Fourier transform infrared spectroscopic approach to the study of the secondary cell wall development in cotton fiber. *Cellulose*, *17*(2), 309–320.

Abidi, N., Hequet, E., & Cabrales, L. (2010). Changes in sugar composition and cellulose content during the secondary cell wall biogenesis in cotton fibers. *Cellulose*, *17*(1), 153–160.

Abidi, N., Hequet, E., Cabrales, L., Gannaway, J., Wilkins, T., & Wells, L. W. (2008). Evaluating cell wall structure and composition of developing cotton fibers using Fourier transform infrared spectroscopy and thermogravimetric analysis. *Journal of Applied Polymer Science*, *107*(1), 476–486.

Akerholm, M., Hinterstoisser, B., & Salmen, L. (2004). Characterization of the crystalline structure of cellulose using static and dynamic FT-IR spectroscopy. *Carbohydrate Research*, *339*(3), 569–578.

Alonso-Simon, A., Garcia-Angulo, P., Melida, H., Encina, A., Alvarez, J. M., & Acebes, J. L. (2011). The use of FTIR spectroscopy to monitor modifications in plant cell

wall architecture caused by cellulose biosynthesis inhibitors. *Plant Signaling & Behaviors*, *6*(8), 1104–1110.
Atalla, R. H., & VanderHart, D. L. (1984). Native cellulose: A composite of two distinct crystalline forms. *Science*, *223*(4633), 283–285.
Carpita, N. C., Defernez, M., Findlay, K., Wells, B., Shoue, D. A., Catchpole, G., & McCann, M. C. (2001). Cell wall architecture of the elongating maize coleoptile. *Plant Physiology*, *127*(2), 551–565.
Chanzy, H., Imada, K., & Vuong, R. (1978). Electron diffraction from the primary wall of cotton fibers. *Protoplasma*, *94*, 299–306.
Chen, L., Wilson, R. H., & McCann, M. C. (1997). Investigation of macromolecule orientation in dry and hydrated walls of single onion epidermal cells by FTIR microspectroscopy. *Journal of Molecular Structure*, *408/409*, 257–260.
Chen, L. M., Carpita, N. C., Reiter, W. D., Wilson, R. H., Jeffries, C., & McCann, M. C. (1998). A rapid method to screen for cell-wall mutants using discriminant analysis of Fourier transform infrared spectra. *Plant Journal*, *16*(3), 385–392.
Dokken, K. M., Davis, L. C., & Marinkovic, N. S. (2005). Use of infrared microspectroscopy in plant growth and development. *Applied Spectroscopy Reviews*, *40*(4), 301–326.
Gokani, S. J., Kumar, R., & Thaker, V. S. (1998). Potential role of abscisic Acid in cotton fiber and ovule development. *Journal of Plant Growth Regulation*, *17*, 1–5.
Haigler, C. H., Betancur, L., Stiff, M. R., & Tuttle, J. R. (2012). Cotton fiber: A powerful single-cell model for cell wall and cellulose research. *Frontiers in Plant Science*, *3*(104), 1–7.
Hu, X. P., & Hsieh, Y. L. (1996). Crystalline structure of developing cotton fibers. *Journal of Polymer Science Part B: Polymer Physics*, *34*(8), 1451–1459.
Huwyler, H. R., Franz, G., & Meier, H. (1979). Changes in the composition of cotton fiber Cell walls during development. *Planta*, *146*, 635–642.
Ilharco, L. M., Garcia, A. R., daSilva, J. L., & Ferreira, L. F. V. (1997). Infrared approach to the study of adsorption on cellulose: Influence of cellulose crystallinity on the adsorption of benzophenone. *Langmuir*, *13*(15), 4126–4132.
Kacurakova, M., Capek, P., Sasinkova, V., Wellner, N., & Ebringerova, A. (2000). FT-IR study of plant cell wall model compounds: Pectic polysaccharides and hemicelluloses. *Carbohydrate Polymers*, *43*, 195–203.
Kohel, R., Richmond, T., & Lewis, C. (1970). Description of a genetic standard for *Gossypium hirsutum* L. *Crop Science*, *10*, 670–674.
Kong, J., & Yu, S. (2007). Fourier transform infrared spectroscopic analysis of protein secondary structures. *Acta Biochimica et Biophysica Sinica*, *39*(8), 549–559.
Krässig, H. A. (1993). *Cellulose structure, accessiblity and reactivity* (2nd ed.). The Netherlands: Gordon and Breach Science Publishers.
Liang, C. Y., & Marchessault, R. H. (1959). Infrared spectra of crystalline polysaccharides. II. Native celluloses in the region 640 to 1700 cm^{-1}. *Journal of Applied Polymer Science*, *39*, 269–278.
Maltby, D., Carpita, N. C., Montezinos, D., Kulow, C., & Delmer, D. P. (1979). β-1,3-Glucan in developing cotton fibers. *Plant Physiology*, *63*, 1158–1164.
McCann, M. C., Hammouri, M., Wilson, R., Belton, P., & Roberts, K. (1992). Fourier-transform infrared microspectroscopy is a new way to look at plant-cell walls. *Plant Physiology*, *100*(4), 1940–1947.
Meinert, M. C., & Delmer, D. P. (1977). Changes in biochemical composition of the cell wall of the cotton fiber during development. *Plant Physiology*, *59*(6), 1088–1097.
Mouille, G., Robin, S., Lecomte, M., Pagant, S., & Hofte, H. (2003). Classification and identification of *Arabidopsis* cell wall mutants using Fourier-transform infrared (FT-IR) microspectroscopy. *Plant Journal*, *35*(3), 393–404.
Nelson, M. L., & Mares, T. (1965). Accessibility and lateral order distribution of the cellulose in the developing cotton fiber. *Textile Research Journal*, *35*, 592–603.
Nelson, M. L., & O'Connor, R. T. (1964). Relation of certain infrared bands to cellulose crystallinity and crystal lattice type. Part II. A new infrared ratio for estimation of crystallinity in cellulose I and II. *Journal of Applied Polymer Science*, *8*, 1325–1341.
Oh, S. Y., Yoo, D. I., Shin, Y., & Seo, G. (2005). FTIR analysis of cellulose treated with sodium hydroxide and carbon dioxide. *Carbohydrate Research*, *340*(3), 417–428.
Oh, S. Y., You, D. I., Shin, Y., Kim, H. C., Kim, H. Y., Chung, Y. S., Park, W. H., & You, J. H. (2005). Crystalline structure analysis of cellulose treated with sodium hydroxide and carbon dioxide by means of X-Ray diffraction and FTIR spectroscopy. *Carbohydrate Research*, *340*, 2376–2391.
Pastorova, I., Botto, R. E., Arisz, P. W., & Boon, J. J. (1994). Cellulose char structure – A combined analytical Py-Gc-Ms, FTIR, and NMR-study. *Carbohydrate Research*, *262*(1), 27–47.
Salmen, L., & Bergstrom, E. (2009). Cellulose structural arrangement in relation to spectral changes in tensile loading FTIR. *Cellulose*, *16*(6), 975–982.
Schwanninger, M., Rodrigues, J. C., Pereira, H., & Hinterstoisser, B. (2004). Effects of short-time vibratory ball milling on the shape of FT-IR spectra of wood and cellulose. *Vibrational Spectroscopy*, *36*(1), 23–40.
Singh, B., Avci, U., Inwood, S. E. E., Grimson, M. J., Landgraf, J., Mohnen, D., Sorensen, I., Wilkerson, C. G., Willats, W. G. T., & Haigler, C. H. (2009). A specialized outer layer of the primary cell wall joins elongating cotton fibers into tissue-like bundles. *Plant Physiology*, *150*(2), 684–699.
Stewart, D., Mcdougall, G. J., & Baty, A. (1995). Fourier-transform infrared microspectroscopy of anatomically different cells of flax (Linum-Usitatissimum) stems during development. *Journal of Agricultural and Food Chemistry*, *43*(7), 1853–1858.
Timpa, J. D., & Triplett, B. A. (1993). Analysis of cell-wall polymers during cotton fiber development. *Planta*, *189*, 101–108.
Tokumoto, H., Wakabayashi, K., Kamisaka, S., & Hoson, T. (2002). Changes in the sugar composition and molecular mass distribution of matrix polysaccharides during cotton fiber development. *Plant and Cell Physiology*, *43*(4), 411–418.
Updegraff, D. M. (1969). Semimicro determination of cellulose in biological materials. *Analytical Biochemsitry*, *32*, 420–424.
Viles, F. J., & Silverman, L. (1949). Determination of starch and cellulose with anthrone. *Analytical Chemistry*, *21*(8), 950–953.
Wada, M., Heux, L., & Sugiyama, J. (2004). Polymorphism of cellulose I family: reinvestigation of cellulose IV_I. *Biomacromolecules*, *5*(4), 1385–1391.
Wilson, R. H., Smith, A. C., Kacurakova, M., Saunders, P. K., Wellner, N., & Waldron, K. W. (2000). The mechanical properties and molecular dynamics of plant cell wall polysaccharides studied by Fourier-transform infrared spectroscopy. *Plant Physiology*, *124*(1), 397–405.
Yan, H. J., Hua, Z. Z., Qian, G. S., Wang, M., Du, G. C., & Chen, J. (2009). Analysis of the chemical composition of cotton seed coat by Fourier-transform infrared (FT-IR) microspectroscopy. *Cellulose*, *16*(6), 1099–1107.